https://doi.org/10.5194/wes-2026-66
Preprint. Discussion started: 23 April 2026

eawe european academy of wind energy
Open Access WIND ENERGY SCIENCE DISCUSSIONS

Dynamic Geostrophic Nudging (DGN): A Novel Method for Controlling the Background Flow in Large Eddy Simulation

Hai Bui[1], Mostafa Bakhoday-Paskyabi[1], and Joachim Reuder[1]

[1]Geophysical Institute and Bergen Offshore Wind Centre, University of Bergen, Norway

Correspondence: Hai Bui (hai.bui@uib.no)

Abstract. Initializing idealized Large-Eddy Simulations (LES) for wind energy applications presents a persistent control problem, typically characterized by slow convergence due to inertial oscillations and the difficulty of matching target height wind targets. To address this, we present Dynamic Geostrophic Nudging (DGN), a method that couples physical fidelity with computational efficiency. Unlike standard velocity nudging, DGN acts on the forcing terms: it dynamically adjusts the geostrophic wind components based on the flow tendency and the error between the mean velocity and the target value. This mechanism allows the controller to efficiently steer the mean wind toward the target while actively damping inertial oscillations in the boundary layer. We employ a one-dimensional model to perform a parameter sweep and investigate the sensitivity of the control parameters before applying the method to a full three-dimensional LES. The results demonstrate that DGN reduces the spin-up time from the standard 12–24 hours to approximately two hours while maintaining the target wind vector with high accuracy. Furthermore, by arresting the unphysical transient growth of the boundary layer, the method allows for the use of vertically optimized domains, representing a significant advancement in the operational efficiency of precursor generation for wind farm simulations.

1 Introduction

Large Eddy Simulation (LES) has established itself as the de facto standard for high-fidelity modeling of the Atmospheric Boundary Layer (ABL), particularly for applications sensitive to turbulence-structure interactions, such as wind farm optimization, pollutant dispersion, and urban canopy flows (Stoll et al., 2020; Meneveau and Katz, 2000; Porté-Agel et al., 2020). While real-world applications increasingly utilize mesoscale-to-microscale coupling (Muñoz-Esparza et al., 2017; Bui et al., 2024), idealized LES remains the primary tool for fundamental process studies and the generation of inflow turbulence. In these idealized frameworks, the meteorological background is typically parameterized via a horizontal pressure gradient force (PGF), represented by a constant geostrophic wind vector, $\mathbf{G} = (U_g, V_g)$ (Moeng, 1984; Wyngaard, 2010).

Despite the simplifying assumptions of idealized Large-Eddy Simulation (LES), initializing these simulations to a specific, statistically stationary state presents a persistent control problem that couples physical fidelity with computational cost (Porté-

https://doi.org/10.5194/wes-2026-66
Preprint. Discussion started: 23 April 2026

eawe european academy of wind energy
Open Access WIND ENERGY SCIENCE DISCUSSIONS

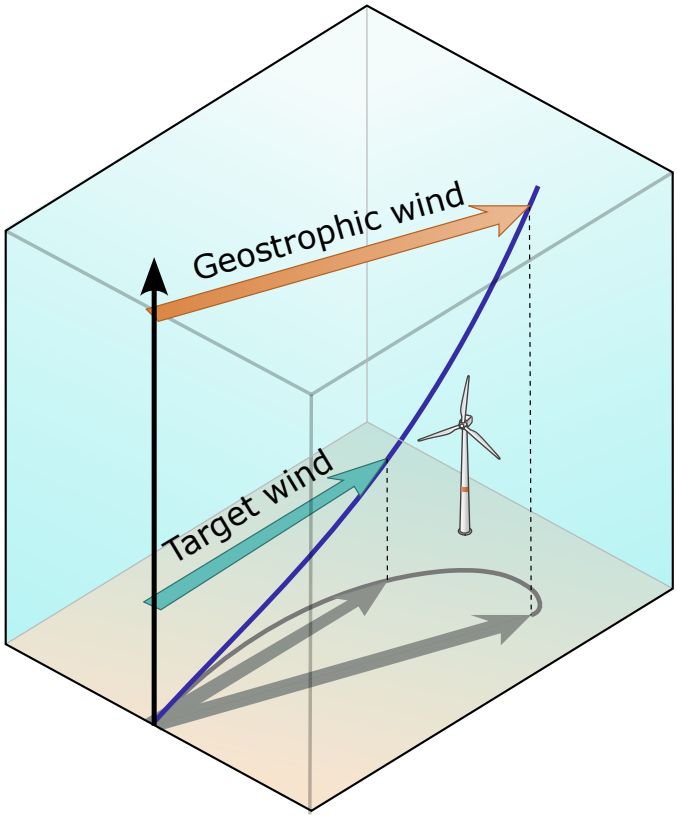

Figure 1. Schematic of the ABL force balance and the resulting control challenge. The geostrophic forcing ($\mathbf{G}$, orange) drives the flow, but due to Coriolis and frictional forces, the realized wind vector rotates and decelerates (grey spiral) as it approaches the surface. This creates a discrepancy in both magnitude and direction between the forcing and the target wind at the target height.

Agel et al., 2020). In a horizontally homogeneous ABL, the equilibrium wind profile is governed by a three-way balance between the large-scale Pressure Gradient Force (PGF), the Coriolis force, and the vertical divergence of turbulent momentum flux (Stull, 2012). This balance generally manifests as a vertical turning of the wind vector (wind veer) and a reduction in magnitude toward the surface—classically described as the Ekman spiral (see Fig. 1) (Garratt, 1994). Consequently, the resulting wind velocity at a specific target height is strictly coupled to surface roughness and thermal stability, rendering it rotated and decelerated relative to the geostrophic forcing $\mathbf{G}$ (Wyngaard, 2010).

Because an arbitrary initial wind profile rarely satisfies this force balance, the system undergoes a prolonged transient adjustment dominated by inertial oscillations (Stull, 2012). These oscillations manifest as a rotation of the momentum vector with a period of $T = 2\pi/f$ (where f is the Coriolis parameter). This physical constraint imposes a heavy toll regardless of the initialization strategy: whether employing a separate periodic precursor simulation or spinning up the primary domain directly. The flow typically requires 12 to 24 hours of physical time to dampen these oscillations and reach the stationary state (Mirocha

https://doi.org/10.5194/wes-2026-66
Preprint. Discussion started: 23 April 2026

eawe european academy of wind energy
Open Access WIND ENERGY SCIENCE DISCUSSIONS

et al., 2014; Bui et al., 2024). Consequently, researchers are forced to discard the majority of the computed solution as spin-up, representing a substantial waste of computational resources.

The long spin-up period creates a further complication related to boundary layer growth. In convective simulations, the turbulent boundary layer deepens continuously due to entrainment at the capping inversion (de Roode et al., 2004). Over a multi-hour initialization, the boundary layer depth can increase so much that it begins to interact with the model top or the upper Rayleigh damping layer, which can contaminate the simulation's statistics. To avoid this, researchers are often forced into expensive compromises, such as using excessively tall vertical domains simply to accommodate this transient growth, or implementing secondary controls, like nudging the potential temperature profile, to artificially limit the boundary layer height (Grylls et al., 2020; Schnierstein et al., 2024). Such artificial temperature controls can create a non-physical state where the boundary layer depth is mismatched with the developed Turbulent Kinetic Energy (TKE). By instead shortening the required spin-up time, DGN allows the system to reach momentum equilibrium before excessive, unphysical boundary layer growth can occur, preserving thermodynamic consistency.

A fundamental challenge in wind energy applications is ensuring that the simulated background flow matches a specific speed and direction at a target height. Because the relationship between the geostrophic forcing $\mathbf{G}$ (the large-scale pressure gradient) and the resulting target height wind is nonlinear and highly dependent on thermal stability, the required forcing is a priori unknown (Stull, 2012). To address this, researchers have historically employed three primary strategies, each with distinct limitations. First, data assimilation techniques (e.g., 4D-Var or Ensemble Kalman Filters) can force the simulation to track observational data; however, these methods are complex to implement (Wrba et al., 2025). Second, Newtonian relaxation is often used to pull the mean flow toward a target profile by adding a source term to the momentum equations (Boyer and Keeler, 2022). While effective at imposing the mean wind, this technique introduces artificial forces that violate the momentum conservation laws and can spuriously dampen the resolved turbulence. Third, researchers may rely on a constant, predetermined forcing $\mathbf{G}$, applied either directly to the primary domain or spun up within a separate, periodic precursor simulation (Mirocha et al., 2014; Bui et al., 2024). This maintains physical consistency but shifts the burden to the initialization phase in which finding the correct $\mathbf{G}$ may requires an expensive trial-and-error process.

To resolve these issues without compromising physical consistency, this paper introduces Dynamic Geostrophic Nudging (DGN), a closed-loop control strategy that acts on the forcing parameters rather than directly modifying the velocity field. By dynamically adjusting the geostrophic wind components based on a feedback law derived from the governing equations, DGN allows turbulence to develop naturally while continuously steering the system toward equilibrium. This approach is designed to effectively dampen inertial oscillations in the boundary layer, thereby minimizing the need for prolonged spin-up periods or excessively deep domains, and ensuring that the final mean flow aligns closely with user-defined targets without the need for manual iterative tuning. The paper is organized as follows: Section 2 details the derivation of the control law, Section 3 provides validation via a reduced-order model, Section 4 demonstrates efficacy in full 3D WRF-LES simulations, and Section 5 summarizes the implications for operational workflows.

https://doi.org/10.5194/wes-2026-66
Preprint. Discussion started: 23 April 2026

eawe european academy of wind energy
Open Access WIND ENERGY SCIENCE DISCUSSIONS

2 Methodology: Dynamic Geostrophic Nudging (DGN)

2.1 Theoretical Formulation

The proposed method controls the horizontally averaged wind by dynamically adjusting the geostrophic wind vector, $\mathbf{G} = (U_g, V_g)$. The core concept is to treat $\mathbf{G}$ not as a static input, but as a control variable that is continuously updated to steer the simulated wind towards a desired target state.

Let the horizontally averaged horizontal wind vector at the target height z_r be $\overline{\mathbf{v}} = (\overline{u}, \overline{v})$. The governing momentum equations, averaged horizontally, can be written in vector form as:

$$\frac{d\overline{\mathbf{v}}}{dt} = f\mathbf{k} \times (\mathbf{G} - \overline{\mathbf{v}}) + \mathbf{F}_{turb} \tag{1}$$

where f is the Coriolis parameter, $\mathbf{k}$ is the vertical unit vector, and $\mathbf{F}_{turb}$ represents the divergence of the vertical turbulent momentum flux.

Our objective is to drive the simulated wind vector $\overline{\mathbf{v}}$ to a user-defined reference vector $\mathbf{v}_r = (u_r, v_r)$. To do this, we define a desired, controlled tendency using a relaxation approach:

$$\left(\frac{d\overline{\mathbf{v}}}{dt}\right)_{\text{target}} = -\frac{\overline{\mathbf{v}} - \mathbf{v}_r}{\tau} \tag{2}$$

where τ is a relaxation timescale. To achieve this target tendency, we introduce a corrective adjustment, $\Delta\mathbf{G}$. The modified governing equation becomes:

$$\left(\frac{d\overline{\mathbf{v}}}{dt}\right)_{\text{target}} = f\mathbf{k} \times ((\mathbf{G} + \Delta\mathbf{G}) - \overline{\mathbf{v}}) + \mathbf{F}_{turb} \tag{3}$$

By equating our desired tendency (Eq. 2) with the physically-forced tendency (Eq. 3) and recognizing the terms from Eq. 1, we simplify:

$$-\frac{\overline{\mathbf{v}} - \mathbf{v}_r}{\tau} = \left(\frac{d\overline{\mathbf{v}}}{dt}\right)_{\text{prior}} + f\mathbf{k} \times (\Delta\mathbf{G}), \tag{4}$$

where the subscription ‘prior’ indicate the tendencies before applying the nudging. Solving for the geostrophic wind correction:

$$\Delta\mathbf{G} = \frac{1}{f}\mathbf{k} \times \left[\left(\frac{d\overline{\mathbf{v}}}{dt}\right)_{\text{prior}} + \frac{\overline{\mathbf{v}} - \mathbf{v}_r}{\tau}\right] \tag{5}$$

In component form, the required adjustments are:

$$\Delta U_g = -\frac{1}{f}\left[\left(\frac{d\overline{v}}{dt}\right)_{\text{prior}} + \frac{\overline{v} - v_r}{\tau}\right] \tag{6}$$

$$\Delta V_g = \frac{1}{f}\left[\left(\frac{d\overline{u}}{dt}\right)_{\text{prior}} + \frac{\overline{u} - u_r}{\tau}\right] \tag{7}$$

https://doi.org/10.5194/wes-2026-66
Preprint. Discussion started: 23 April 2026

eawe european academy of wind energy
Open Access WIND ENERGY SCIENCE DISCUSSIONS

It is crucial to distinguish this approach from standard Newtonian relaxation (direct nudging) of the velocity field. Unlike direct nudging, which typically applies a corrective force proportional only to the instantaneous velocity error, the proposed geostrophic adjustment (Eqs. 6–7) explicitly incorporates the system current tendency, which has the effect of damping the inertial oscillation. Furthermore, the derivation highlights the inherent rotational coupling imposed by the Coriolis force: the correction for the zonal geostrophic wind component ΔU_g is driven primarily by the error in the meridional wind component $(\overline{v}-v_r)$, and vice versa. This cross-dependence ensures that the applied forcing respects the force balance in the boundary layer, rather than treating the horizontal velocity components as independent scalar quantities. It should be noted that the presence of the $1/f$ factor restricts this formulation to domains with a non-zero Coriolis parameter. Near the equator, the controller would become mathematically unstable. However, because the fundamental phenomena addressed by DGN—Coriolis-induced Ekman veer and prolonged inertial oscillations—are inherently extratropical features, the method is perfectly suited for mid- to high-latitude simulations, which encompass the vast majority of wind energy applications.

2.2 Practical Implementation for Turbulent Flows

In a turbulent simulation such as an LES, the instantaneous horizontally averaged wind $\overline{\mathbf{v}}(z_r)$ is not a smooth variable but is contaminated with high-frequency fluctuations. A direct application of Eqs. (6)-(7) would cause the controller to react to this turbulent noise which, when amplified by the $1/f$ term, leads to large, unphysical oscillations in $\mathbf{G}$.

To ensure robustness, the controller must act on a filtered signal representing the mean state. This is achieved through two mechanisms:

Signal Smoothing.

We apply an Exponential Moving Average (EMA) filter to the wind at the reference height at every model timestep, Δt. The smoothed wind, $\overline{\mathbf{v}}_{\text{smooth}}$, is updated as:

$$\overline{\mathbf{v}}^{n}_{\text{smooth}} = \alpha \cdot \overline{\mathbf{v}}^{n} + (1-\alpha) \cdot \overline{\mathbf{v}}^{n-1}_{\text{smooth}} \tag{8}$$

where the smoothing factor $\alpha = \Delta t / T_{\text{smooth}}$, and T_{smooth} is a user-defined timescale.

Periodic Updates and Tendency Calculation.

The controller updates $\mathbf{G}$ periodically at an interval T_{filter}. The "current tendency" term, inaccessible in a complex model, is approximated using the change in the *smoothed* wind over this interval:

$$\left(\frac{d\overline{\mathbf{v}}}{dt}\right)_{\text{current}} \approx \frac{\overline{\mathbf{v}}^{\text{now}}_{\text{smooth}} - \overline{\mathbf{v}}^{\text{past}}_{\text{smooth}}}{T_{\text{filter}}} \tag{9}$$

The error term, $(\overline{\mathbf{v}} - \mathbf{v}_r)/\tau$, is also calculated using the most recent smoothed value, $\overline{\mathbf{v}}^{\text{now}}_{\text{smooth}}$. This ensures the controller's decision is based entirely on a filtered, stable signal.

https://doi.org/10.5194/wes-2026-66
Preprint. Discussion started: 23 April 2026

eawe european academy of wind energy
Open Access WIND ENERGY SCIENCE DISCUSSIONS

3 Idealized 1D Model Experiments

The implementation of DGN relies on three governing parameters: the relaxation timescale (τ), the exponential smoothing window (T_{smooth}), and the forcing update interval (T_{filter}). Calibrating these parameters is essential to ensure the controller effectively steers the mean wind and damps inertial oscillations without inducing instability. However, performing a systematic parameter sweep is computationally prohibitive in full three-dimensional LES. Therefore, to demonstrate the DGN method and examine its sensitivity to control parameters, we first employ a simple one-dimensional (1D) column model. This allows for rapid, systematic sensitivity experiments to identify robust operating parameters at a negligible computational cost prior to implementation in the 3D solver.

3.1 Model Description

The 1D model simulates the temporal evolution of the horizontally averaged wind profile, $\overline{\mathbf{v}}(z,t) = (\overline{u}, \overline{v})$, governed by the Reynolds-averaged Navier-Stokes equations under the assumption of horizontal homogeneity. The deterministic evolution is given by:

$$\frac{\partial \overline{u}}{\partial t} = f(\overline{v} - V_g) + \frac{\partial}{\partial z}\left(K_m \frac{\partial \overline{u}}{\partial z}\right) \tag{10}$$

$$\frac{\partial \overline{v}}{\partial t} = -f(\overline{u} - U_g) + \frac{\partial}{\partial z}\left(K_m \frac{\partial \overline{v}}{\partial z}\right) \tag{11}$$

where f is the Coriolis parameter and $\mathbf{G} = (U_g, V_g)$ is the geostrophic wind vector, which serves as the time-dependent control variable. A constant eddy viscosity K_m was chosen specifically to reproduce the classical Ekman spiral as the analytical equilibrium solution. Expressing the wind and forcing as complex variables ($\overline{\mathbf{v}} = \overline{u} + i\overline{v}$ and $\mathbf{G} = U_g + iV_g$), the analytical solution is:

$$\overline{\mathbf{v}}(z) = \mathbf{G}\left[1 - e^{-(1+i)z/\delta}\right] \tag{12}$$

or in component form:

$$\overline{u}(z) = U_g - e^{-z/\delta}\left[U_g \cos\left(\frac{z}{\delta}\right) + V_g \sin\left(\frac{z}{\delta}\right)\right] \tag{13}$$

$$\overline{v}(z) = V_g - e^{-z/\delta}\left[V_g \cos\left(\frac{z}{\delta}\right) - U_g \sin\left(\frac{z}{\delta}\right)\right], \tag{14}$$

where $\delta = \sqrt{2K_m/f}$ is the Ekman layer depth. In this study, we select $K_m = 1.0$ m^2 s^{-1} (with $f = 10^{-4}$ s^{-1}), which yields $\delta \approx 141$ m and an effective boundary layer height of $h \approx \pi\delta \approx 444$ m.

To approximate the inherent variability of the mean flow in a 3D LES, a stochastic perturbation term, $\Delta\overline{\mathbf{v}}_{\text{noise}}$, is added to the velocity field after each time step (see Appendix A for details). Boundary conditions consist of a no-slip condition at the surface ($\overline{u} = \overline{v} = 0$ at $z = 0$) and a zero-gradient condition at the model top. To prevent unphysical reflection of disturbances, a Rayleigh damping layer (sponge layer) is applied above a specified height H_{nudge} to relax the velocity toward the geostrophic wind.

https://doi.org/10.5194/wes-2026-66
Preprint. Discussion started: 23 April 2026

eawe european academy of wind energy
Open Access WIND ENERGY SCIENCE DISCUSSIONS

Furthermore, this analytical framework allows us to derive the exact geostrophic forcing required to achieve a specific target. For a target mean wind vector $\overline{\mathbf{v}}_r$ at a reference height z_r, the required geostrophic wind $\mathbf{G}_r$ is determined by inverting Eq. (12):

$$\mathbf{G}_r = \frac{\overline{\mathbf{v}}_r}{1 - e^{-(1+i)z_r/\delta}}. \tag{15}$$

In more comprehensive models such as LES, an exact analytical solution is not possible. However, if we assume the system preserves the shape of the vertical hodograph, the required forcing can be estimated from a converged state. If a simulation driven by an initial guess $\mathbf{G}_0$ converges to a target height velocity $\tilde{\mathbf{v}}$, the adjusted forcing $\mathbf{G}_r$ required to match the target $\mathbf{v}_r$ can be estimated via a complex scaling (see Appendix A for details):

$$\mathbf{G}_r = \left(\frac{\mathbf{v}_r}{\tilde{\mathbf{v}}}\right)\mathbf{G}_0 \tag{16}$$

3.2 Sensitivity Experiments

The efficacy of the DGN controller is governed by three primary tuning parameters: the relaxation timescale (τ), the controller update interval (T_{filter}), and the EMA filter timescale (T_{smooth}). Preliminary tests indicated that the controller's performance is most sensitive to τ and T_{filter}, while being less sensitive to the precise value of the EMA filter, provided it is sufficient to smooth high-frequency noise. Therefore, we fixed T_{smooth} at a physically reasonable value of 10 minutes, a common timescale for meteorological averaging, to focus the main analysis on the more critical parameters.

To identify the optimal configuration of τ and T_{filter}, we then performed an ensemble-based parameter sweep. A matrix of simulations was conducted with T_{filter} varying from 10 to 90 minutes and τ varying from 40 to 120 minutes. This 9×9 matrix was repeated 20 times with different random seeds for the stochastic noise, yielding a total of 1,620 simulations. The fixed physical and numerical parameters for this ensemble are detailed in Table 1.

Performance was evaluated over the final 18 hours of each 24-hour simulation using two metrics. First, Target Wind Error ($\varepsilon_{\mathbf{v}}$) is defined as the Root Mean Square Error (RMSE) of the target height wind speed relative to the target vector $\mathbf{v}_r$. Second, Forcing Convergence Error ($\varepsilon_{\mathbf{G}}$) is defined as the RMSE of the controlled geostrophic wind relative to the analytical solution $\mathbf{G}_r$ (Eq. 15), which is $(12.67, -6.49)$ m/s in this case. Using the analytical solution as a reference provides a rigorous measure of physical fidelity; a successful controller must not only hit the target wind speed but also converge to the correct large-scale forcing required to sustain it.

We defined a combined cost function J to balance these competing objectives:

$$J = 0.5 \cdot \frac{\varepsilon_{\mathbf{v}}}{\max(\varepsilon_{\mathbf{v}})} + 0.5 \cdot \frac{\varepsilon_{\mathbf{G}}}{\max(\varepsilon_{\mathbf{G}})} \tag{17}$$

where the errors are normalized by the maximum values observed in the ensemble to ensure equal weighting.

The results reveal a distinct trade-off between tracking speed and physical convergence (Fig. 2). Aggressive control (low τ, low T_{filter}) yields low tracking error $\varepsilon_{\mathbf{v}}$ (Fig. 2a) but results in a noisy forcing term that fails to settle on the analytical solution, leading to high $\varepsilon_{\mathbf{G}}$ (Fig. 2b). Conversely, passive control (high τ) ensures a stable $\mathbf{G}$ but allows the wind to drift from the

https://doi.org/10.5194/wes-2026-66
Preprint. Discussion started: 23 April 2026

eawe european academy of wind energy
Open Access WIND ENERGY SCIENCE DISCUSSIONS

Table 1. Physical and numerical parameters for the 1D model experiments.

Parameter	Symbol	Value
Coriolis Parameter	f	1×10^{-4} s^{-1}
Eddy Viscosity	K_m	1.0 m^2 s^{-1}
Reference Height (Target)	z_r	100 m
Target Wind Vector	$\mathbf{v}_r$	$(10, 0)$ m/s
Initial Geostrophic Wind	$\mathbf{G}_0$	$(10, 0)$ m/s
Stochastic Intensity	σ_v	0.01 m s$^{-3/2}$
ABL Height	z_i	800 m
Rayleigh Damping Height	H_{nudge}	800 m
Rayleigh Damping Timescale	T_{nudge}	3600 s
EMA Filter Timescale	T_{smooth}	600 s
Model Timestep	Δt	10 s
Data Output Interval	-	60 s

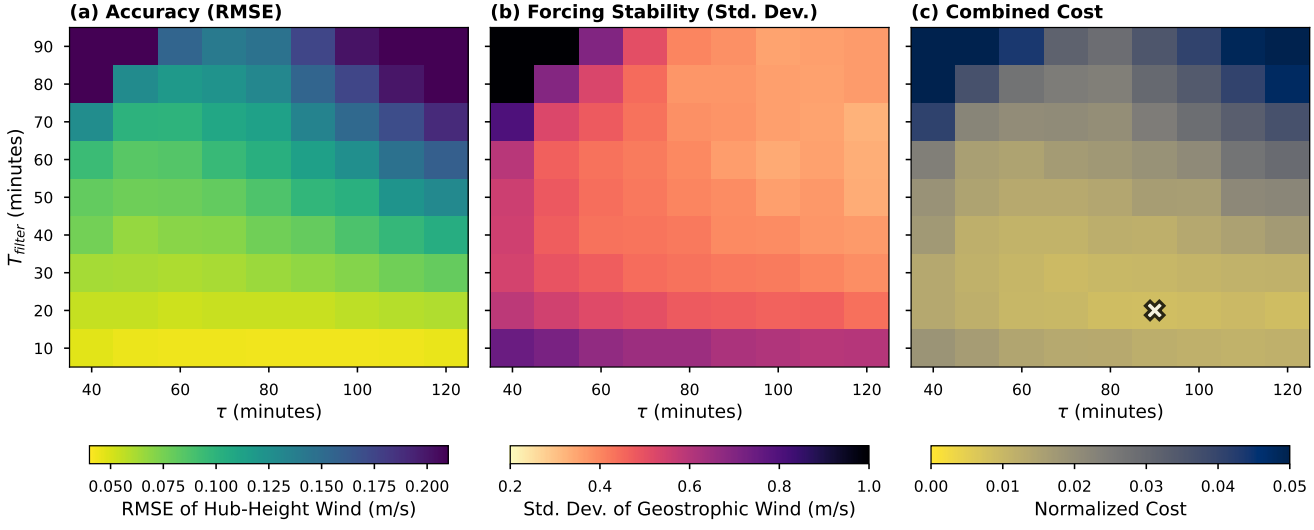

Figure 2. Ensemble-averaged controller performance. (a) Wind Tracking Error ($\varepsilon_{\mathbf{v}}$): RMSE of the target height wind against the target. (b) Forcing Convergence Error ($\varepsilon_{\mathbf{G}}$): RMSE of the geostrophic wind against the analytical Ekman solution. (c) Combined cost metric J. The minimum (marked by 'X') indicates the optimal parameter set balancing accuracy and physical fidelity.

target. Guided by the minimum of the cost function (Fig. 2c), we selected $\tau = 60$ min and $T_{\text{filter}} = 30$ min (marked by 'X') as the robust configuration for subsequent experiments.

https://doi.org/10.5194/wes-2026-66
Preprint. Discussion started: 23 April 2026

eawe european academy of wind energy
Open Access WIND ENERGY SCIENCE DISCUSSIONS

3.3 Comparison of Control Strategies

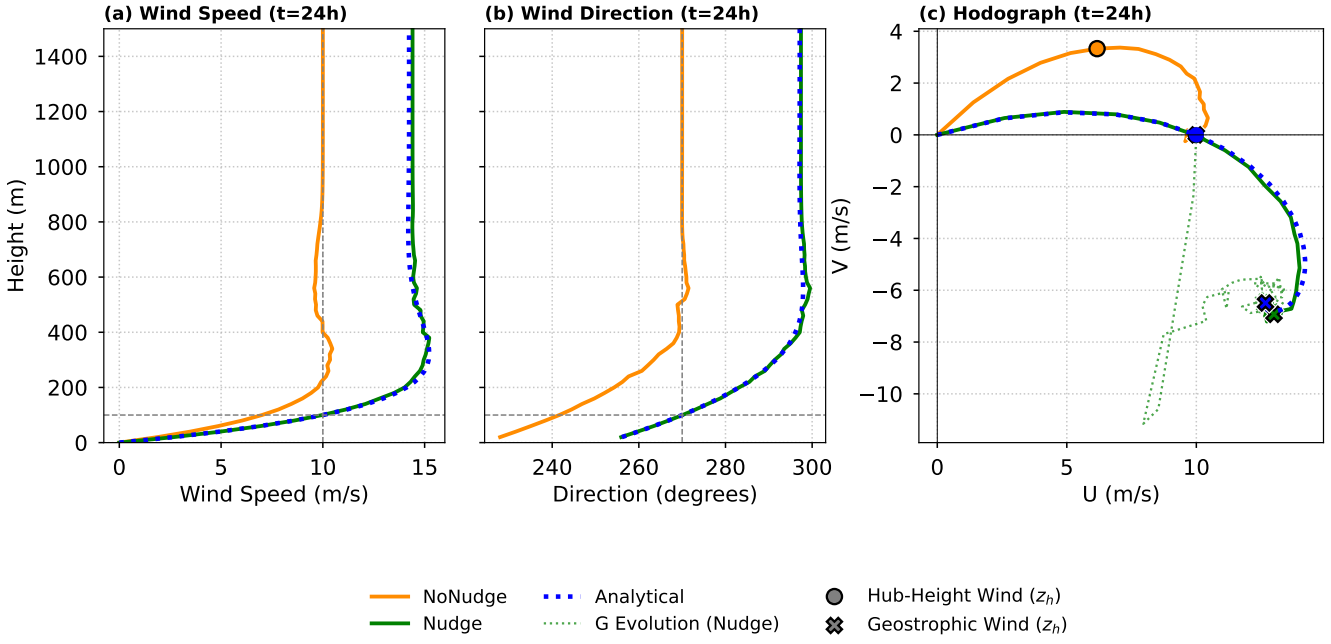

Figure 3. Comparison of the final (t=24h) state for the `NoNudge`, `Nudge`, and Analytical Ekman cases. (a) Wind speed profiles. (b) Wind direction profiles. (c) Hodographs of the wind profiles. Circles mark the wind at the 100 meter reference height, and 'X' markers indicate the final geostrophic wind. The `Nudge` simulation successfully converges to the theoretical analytical solution, while the `NoNudge` simulation exhibits a large steady-state error.

Having established an optimal parameter set for the DGN controller, we now conduct a final comparison to demonstrate its performance against the standard simulation approach and the theoretical solution. We compare three distinct cases:

- `NoNudge`: A baseline simulation where the geostrophic wind, $\mathbf{G}$, is held constant at the target velocity, $(10, 0)$ m/s.
- `Nudge`: The dynamically controlled simulation, where the DGN method is applied using the optimal set of parameters identified in the sensitivity study.
- `Analytical`: The theoretical steady-state solution given by Eq. (12), where the required geostrophic wind, $\mathbf{G}_r$, is calculated a priori from the inverse Ekman formula (Eq. 15). This serves as the ground truth for the final equilibrium state.

Figure 3 presents the final state of the boundary layer after 24 hours of simulation, comparing the results of the two numerical experiments to the analytical solution. The `NoNudge` simulation clearly demonstrates the fundamental problem with a naive forcing strategy. Due to the Ekman spiral effect, its final wind profile (orange dashed line) fails to achieve the target wind speed

https://doi.org/10.5194/wes-2026-66
Preprint. Discussion started: 23 April 2026

eawe european academy of wind energy
Open Access WIND ENERGY SCIENCE DISCUSSIONS

or direction at the 100-m reference height. The corresponding target height wind marker (orange circle) on the hodograph is far from the desired state of $(10, 0)$ m/s.

In contrast, the final profile from the `Nudge` simulation (solid green line) is in excellent agreement with the theoretical Analytical Ekman solution (dotted blue line) across the entire boundary layer depth. As shown in all three panels, the controller has successfully forced the simulation to converge to the physically correct steady state. On the hodograph in panel (c), the target height wind marker for the `Nudge` case (green circle) lies precisely on the target, perfectly matching the analytical solution's marker (black circle).

Most critically, panel (c) visualizes the action of the controller. The dotted green line shows the evolution of the geostrophic wind, $\mathbf{G}(t)$, as determined by the DGN method. It starts at the naive guess of $(10, 0)$ m/s and autonomously spirals towards the final, correct geostrophic wind required to balance the flow. This final value (green 'X') is in remarkable agreement with the theoretical geostrophic wind (blue 'X') calculated from the inverse Ekman formula. This result shows that the DGN method not only achieves the correct final state but also automatically discovers the necessary theoretical forcing without any manual tuning.

The analysis of the final profiles in Fig. 3 demonstrates that the DGN method successfully converges the simulation to the theoretically correct equilibrium state. However, the most significant advantage of the method is not just its final accuracy, but the efficiency with which it reaches that state. To illustrate this, Figure 4 directly compares the transient behavior and spin-up time of the `NoNudge` and `Nudge` cases over the full 24-hour period.

The `NoNudge` case (orange line) clearly illustrates the problem of a prolonged spin-up. Starting from a state of force imbalance, the flow develops a large-amplitude inertial oscillation. As seen in panels (a) and (b), the target height wind speed undershoots to nearly 6 m/s, and the direction over-rotates to about 240° after approximately 8 hours. The system then slowly oscillates back, but has still not settled on a stable equilibrium even after 24 hours.

In contrast, the `Nudge` case (green line) demonstrates the primary benefit of the DGN method. By continuously adjusting the geostrophic wind, the controller actively damps the inertial oscillation. Panels (a) and (b) show that it rapidly steers the target height wind to the target state, converging smoothly to the 10 m/s speed and 270° direction in approximately 2 hours and maintaining it with high precision for the remainder of the simulation.

Panel (c) reveals the mechanism behind this rapid convergence. The `NoNudge` case is forced with a constant, incorrect geostrophic wind. The `Nudge` case, however, dynamically adjusts the forcing. Starting from the naive guess of $(10, 0)$ m/s, the controller smoothly drives the geostrophic wind components towards their final, correct equilibrium values. After approximately 5 hours, the controller's applied forcing (dashed and dotted green lines) has autonomously converged to the theoretical analytical values (blue lines). This automated adjustment is what suppresses the physical force imbalances that cause the long-period oscillations, effectively eliminating the computationally expensive spin-up period.

https://doi.org/10.5194/wes-2026-66
Preprint. Discussion started: 23 April 2026

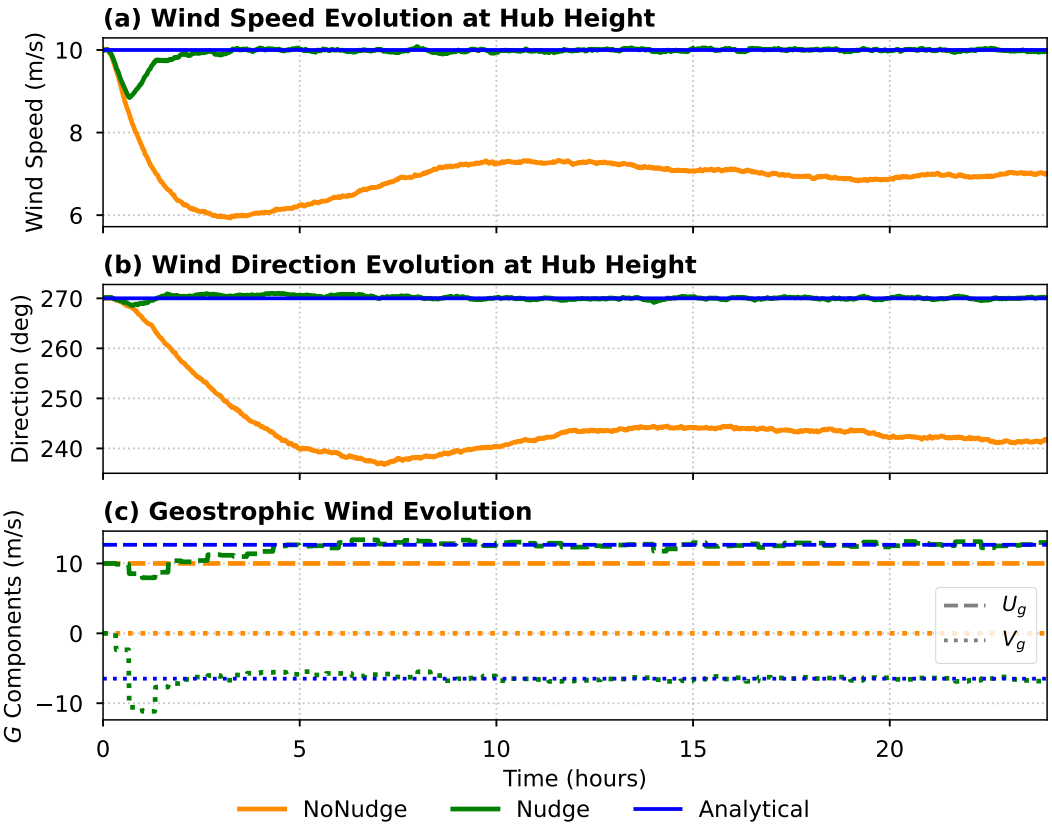

Figure 4. Time series comparison for the 1D model simulations. (a) Wind speed at the 100-m reference height. (b) Wind direction at the target height. (c) Evolution of the applied geostrophic wind components. The 'Analytical' lines in panel (c) show the theoretical geostrophic wind components required to achieve the target state.

4 Validation in a 3D LES Environment

Having demonstrated the concept and explored the parameter sensitivity of the DGN method in an idealized 1D model, we now validate its performance in a full 3D Large-Eddy Simulation. The objective is to confirm that the method is effective in a realistic, stochastic turbulent environment and to illustrate its practical benefits for generating on-target inflow conditions.

4.1 WRF-LES Configuration

The 3D simulations were performed using the Weather Research and Forecasting model (WRF, version 4.3.1; Skamarock et al., 2019), configured for idealized LES. The DGN method was implemented within the WRF-SADLES framework (V2.0b; Bui et al., 2024; Bui, 2026a), which is designed for wind energy applications. The LES mode is enabled using the standard 1.5-order three-dimensional Turbulent Kinetic Energy (TKE) closure scheme (Lilly, 1967).

https://doi.org/10.5194/wes-2026-66
Preprint. Discussion started: 23 April 2026

eawe european academy of wind energy
Open Access WIND ENERGY SCIENCE DISCUSSIONS

The simulation was conducted on a doubly periodic domain with a horizontal extent of 2.4×1.2 km and a vertical extent of 1.2 km, using an isotropic grid resolution of $\Delta x = \Delta y = \Delta z = 20$ m. All simulations were run for 24 hours with a timestep of 0.2 s, and output was saved every 10 minutes. The Coriolis parameter was set to $f = 1.177 \times 10^{-4}$ s^{-1}. Surface fluxes were calculated using the Revised MM5 Monin-Obukhov surface layer scheme (Jiménez et al., 2012) with a surface roughness length of 1 mm. To drive the development of a convective boundary layer, a constant kinematic surface sensible heat flux of $(\overline{w'\theta'})_s = 0.024$ K m s^{-1} is prescribed, corresponding to weakly convective conditions (Kale et al., 2022; Bui et al., 2024). All other physics parameterizations (e.g., microphysics, radiation) were deactivated, and a Rayleigh damping layer was applied to the top 300 m of the domain to prevent spurious wave reflections.

Consistent with the 1D model study, two primary simulations were conducted:

- `NoNudge`: A baseline simulation with a fixed geostrophic wind set equal to the target wind, $\mathbf{G} = (10, 0)$ m/s.
- `Nudge`: A simulation where the DGN method is applied. The controller parameters were set to the values identified in the 1D sensitivity study: $\tau = 90$ minutes, $T_{\text{filter}} = 20$ minutes, and $T_{\text{smooth}} = 5$ minutes, with the target level set to a height of approximately 100 m ($k = 5$).

It is important to note that while these parameters were optimal for the simplified 1D model, they are not guaranteed to be the absolute optimum for the more complex 3D LES environment. A full parameter optimization for 3D simulations is a substantial undertaking and is considered beyond the scope of this study. Instead, a key objective of this work is to use these 1D-derived parameters as a rational starting point and thereby demonstrate the robustness and transferability of the DGN tuning process. The goal is to illustrate the method's effectiveness even when not perfectly optimized for the specific 3D turbulent state.

4.2 Simulation Results and Analysis

The primary result of the 3D validation is presented in Figure 5, which directly comparing the spin-up behavior of the two simulations. The results are remarkably consistent with the idealized 1D model findings. The `NoNudge` case (orange line) clearly demonstrates the characteristic inertial oscillation. This is most evident in the wind speed (panel a), which first undershoots to approximately 8.5 m/s near hour 2.5 (1.5 m/s off the target), before recovering and overshooting to a peak of nearly 10.5 m/s around hour 10. The wind direction (panel b) exhibits a similar oscillatory behavior, with a large initial excursion to the left, reaching a minimum of approximately 255 degrees (15 degrees to the left of the target) between hours 8 and 10. Although the amplitude of the oscillation damps significantly over the 24-hour period, the system is still slowly evolving and has not yet reached a complete steady-state equilibrium by the end of the simulation.

In contrast, the `Nudge` case (green line) demonstrates the controller's effectiveness in this fully turbulent environment. The DGN method successfully suppresses the large-scale inertial oscillation, keeping both the wind speed and direction centered around the target values throughout the simulation. The variability in both wind speed and direction is larger than in the idealized 1D case. This is likely attributable to the explicitly resolved, domain-scale turbulent structures in the 3D LES, which are only represented by a simple stochastic model in 1D.

https://doi.org/10.5194/wes-2026-66
Preprint. Discussion started: 23 April 2026

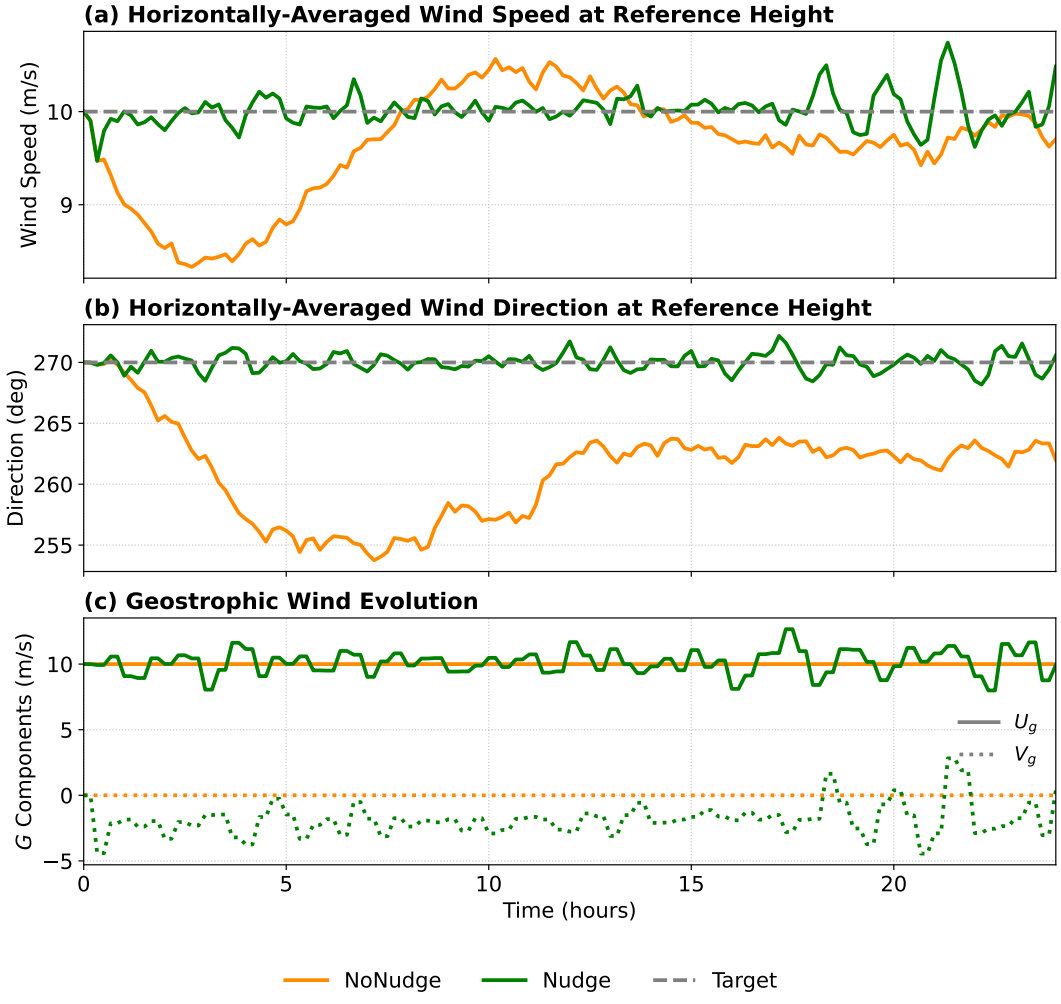

Figure 5. Time series comparison for the 3D WRF-LES simulations. (a) Horizontally-averaged wind speed at the reference height (100 m). (b) Horizontally-averaged wind direction. (c) Evolution of the applied geostrophic wind components. The DGN method (`Nudge`) effectively eliminates the long spin-up period at the target height.

A closer inspection of the `Nudge` time series reveals a distinct evolution in this variability. To quantify this, we divided the 24-hour period into three consecutive 8-hour windows. The standard deviation of the reference-height wind speed decreases from 0.14 m/s in the initial window (0–8h) to a of 0.08 m/s in the middle window (8–16h), consistent with the controller reaching a stable operating state after the initial adjustment. However, a significant increase in variability is observed in the final window (16–24h), where the standard deviation triples to 0.25 m/s. This late-stage increase suggests a change in the physical state of the simulated boundary layer, which will be investigated in the subsequent analysis.

https://doi.org/10.5194/wes-2026-66
Preprint. Discussion started: 23 April 2026

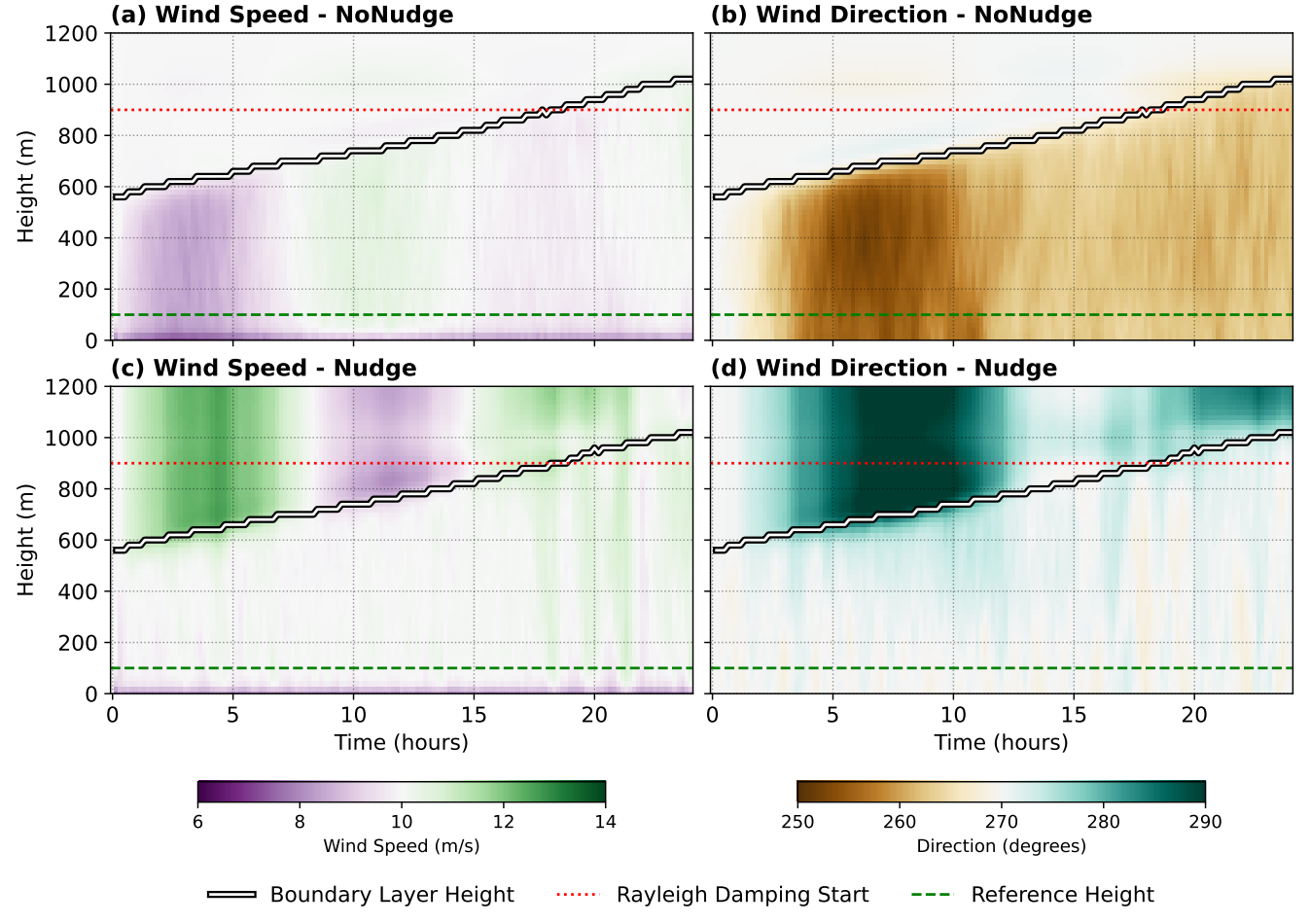

Figure 6. Time-height evolution of horizontally-averaged wind speed (a, c) and wind direction (b, d) for the `NoNudge` and `Nudge` simulations. The Boundary Layer Height (solid line with black outline), the start of the Rayleigh damping layer (red dotted line), and the reference height (green dashed line) are overlaid.

https://doi.org/10.5194/wes-2026-66
Preprint. Discussion started: 23 April 2026

eawe european academy of wind energy
Open Access WIND ENERGY SCIENCE DISCUSSIONS

A crucial test of the DGN method is whether it achieves control without artificially altering the physical turbulence structure. Figure 7 compares the turbulence evolution and statistics between the `Nudge` and `NoNudge` simulations. The time-height evolution of Turbulence Kinetic Energy (TKE) in panels (a) and (b) is visually similar. In both cases, turbulence initiates at the surface and the turbulent layer deepens in concert with the growing boundary layer, providing qualitative evidence that the DGN controller does not suppress the physical development of turbulence.

This is confirmed quantitatively in panel (c), which shows the TKE profiles averaged over a mature period (10–15h). The vertical structure of the turbulence is well-preserved, with both simulations showing the canonical shape for a CBL, including a peak in the lower half of the boundary layer. While the ensemble-averaged TKE in the `Nudge` case is marginally larger than in the baseline simulation, the difference is small, particularly near the reference height. Overall, this analysis demonstrates that the DGN controller successfully manipulates the mean flow without compromising the fundamental physical realism of the simulated turbulence.

5 Conclusion

The initialization of idealized Large Eddy Simulations of the atmospheric boundary layer presents a persistent challenge. The standard method of applying a constant geostrophic wind requires long, computationally expensive spin-up periods to overcome inertial oscillations and a laborious trial-and-error process to achieve specific wind conditions at a target height. This paper introduced and validated a novel method, Dynamic Geostrophic Nudging (DGN), which treats the geostrophic wind as a dynamic control variable to solve these long-standing issues.

The DGN method is based on a feedback control law derived directly from the horizontally-averaged momentum equations. By incorporating both the instantaneous error from a target state and the tendency of the mean wind, the controller actively damps inertial oscillations and continuously adjusts the large-scale forcing to steer the system toward the desired equilibrium. The method's efficacy was first established in an idealized 1D model, which provided a proof of concept and was used to conduct a systematic, ensemble-based parameter sweep. This analysis provided crucial insight into the controller's behavior and identified a robust set of tuning parameters. The 1D results demonstrated that the DGN method not only rapidly converges to the correct final state but also autonomously discovers the theoretical geostrophic forcing required to maintain it.

The primary contribution of this work was the successful implementation and validation of the DGN method in a full 3D LES of a convective boundary layer. The results from the 3D simulations were in excellent agreement with the 1D model findings. The DGN controller, using parameters derived from the simple 1D study, successfully eliminated the multi-hour inertial oscillation, achieving a quasi-equilibrium, on-target state. Furthermore, a detailed analysis of the turbulence structure confirmed that the DGN method performs its function without artificially altering the physical development or statistical properties of the simulated turbulence.

The proposed DGN method offers significant advantages for the atmospheric modeling community. By rapidly achieving a stable, on-target state, it drastically reduces the computational cost associated with long spin-up phases. It provides an automated and robust way to achieve specific, reproducible inflow conditions without manual tuning. This rapid convergence

https://doi.org/10.5194/wes-2026-66
Preprint. Discussion started: 23 April 2026

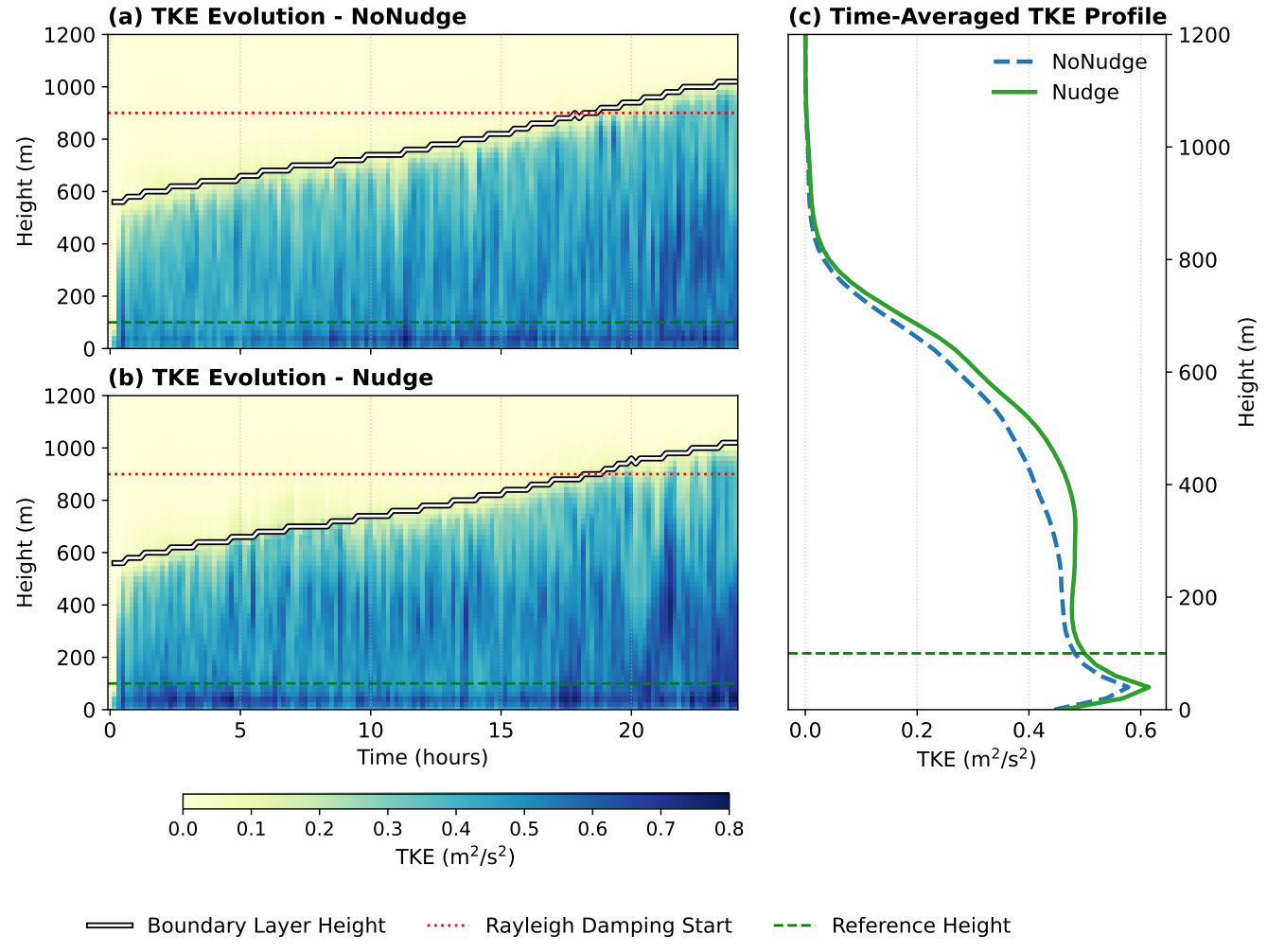

Figure 7. Validation of the turbulence structure. (a) Time-height evolution of TKE for the `NoNudge` simulation. (b) Time-height evolution of TKE for the `Nudge` simulation. (c) Time-averaged profiles of horizontally-averaged TKE for both cases, calculated over the period t=10-15h. The excellent agreement confirms the physical fidelity of the controlled simulation.

also enables a more efficient simulation strategy, allowing for the use of shallower, computationally cheaper domains by obviating the need to accommodate many hours of boundary layer growth. While this study focused on wind energy, the implications are broader, offering benefits to any field that relies on idealized ABL simulations, including air quality, pollutant dispersion, and urban meteorology.

A limitation of the current study, and a key avenue for future research, is the rigorous tuning of the controller parameters for 3D LES under different atmospheric stability conditions. While we have demonstrated that the parameters derived from the 1D model are effective for the weakly convective 3D case, the residual variability in the hub-height wind is noticeably larger than

https://doi.org/10.5194/wes-2026-66
Preprint. Discussion started: 23 April 2026

eawe european academy of wind energy
Open Access WIND ENERGY SCIENCE DISCUSSIONS

in the idealized model. This suggests that a different, truly optimal parameter set likely exists for the full 3D environment, and that this set may be dependent on the specific stability condition. A comprehensive parameter optimization for various stability regimes, while computationally intensive, is an important next step. Additionally, while this study focuses on reaching a single, stationary target equilibrium, the DGN framework could potentially be extended to track time-varying targets, such as diurnal cycles or shifting synoptic conditions. However, the controller's effectiveness in such scenarios will likely depend on the rate of change of the target vectors, which requires further investigation. Nonetheless, the DGN method, even with a non-optimized parameter set derived from a simplified proxy model, has been shown to be a robust and significant step towards more efficient, accurate, and reproducible idealized Large Eddy Simulations.

Code availability. A demonstration of the DGN method in an idealized 1D column model is available on Zenodo (Bui, 2026b). The full 3D implementation of DGN integrated within the WRF-SADLES framework (v2.0b), is also publicly archived on Zenodo (Bui, 2026a).

Appendix A: Derivation of the Manual Geostrophic Wind Correction

This appendix details the derivation of the scaling law used to estimate the corrected geostrophic wind, $\mathbf{G}_r$, for the static benchmark cases. The method assumes that the relationship between the applied geostrophic wind and the resulting equilibrium target height wind can be approximated as a linear, conformal mapping (i.e., a uniform scaling and rotation), which is consistent with the Ekman response in a neutral or stable boundary layer.

To derive the correction, we represent the 2D horizontal vectors as complex variables. Let the geostrophic wind be denoted by $\mathbf{G} = U_g + iV_g$ and the target height mean wind by $\overline{\mathbf{v}} = \overline{u} + i\overline{v}$.

We assume the atmospheric boundary layer acts as a complex linear operator λ, such that

$$\overline{\mathbf{v}} = \lambda \mathbf{G}. \tag{A1}$$

If, from a first guess $\mathbf{G}_0$, we obtain a converged target height wind $\tilde{\mathbf{v}}$, then the system operator λ is empirically determined as

$$\lambda = \frac{\tilde{\mathbf{v}}}{\mathbf{G}_0}. \tag{A2}$$

Our objective is to find the corrected geostrophic forcing $\mathbf{G}_r$ required to produce the user-defined target wind $\mathbf{v}_r$. Assuming λ remains constant, we have

$$\mathbf{v}_r = \lambda \mathbf{G}_r. \tag{A3}$$

Substituting λ gives

$$\mathbf{G}_r = \frac{\mathbf{v}_r}{\lambda} = \frac{\mathbf{v}_r}{\tilde{\mathbf{v}}/\mathbf{G}_0} = \mathbf{G}_0 \left(\frac{\mathbf{v}_r}{\tilde{\mathbf{v}}} \right). \tag{A4}$$

The same transformation corresponds to a rotation–scaling matrix:

$$\begin{pmatrix} U_{gr} \\ V_{gr} \end{pmatrix} = \begin{pmatrix} a & -b \\ b & a \end{pmatrix} \begin{pmatrix} U_{g0} \\ V_{g0} \end{pmatrix}, \tag{A5}$$

https://doi.org/10.5194/wes-2026-66
Preprint. Discussion started: 23 April 2026

eawe european academy of wind energy
Open Access WIND ENERGY SCIENCE DISCUSSIONS

with $a = \frac{v_r\tilde{u}+v_r\tilde{v}}{\tilde{u}^2+\tilde{v}^2}$, $\quad b = \frac{v_r\tilde{u}-v_r\tilde{v}}{\tilde{u}^2+\tilde{v}^2}$.

Appendix B: Justification for the Stochastic Forcing Scaling

This appendix provides the physical justification for scaling the stochastic perturbation, or "kick," by the square root of the model timestep, $\sqrt{\Delta t}$. This scaling is essential for ensuring the numerical implementation of the stochastic process is physically consistent and independent of the choice of Δt.

The stochastic term is formulated to represent the continuous injection of TKE into the resolved flow by unresolved, random turbulent processes. Let the average rate of this stochastic TKE injection per unit mass be a physical constant, ϵ_s, which has units of energy per unit time (m^2/s^3).

The expected amount of energy added to the system during a single model timestep of duration Δt is therefore proportional to the rate multiplied by the duration:

$$\text{Energy added per step} \propto \epsilon_s \Delta t \tag{B1}$$

Kinetic energy is proportional to velocity squared. Therefore, the change in energy is proportional to the change in variance of the velocity, $\text{Var}(\Delta \mathbf{v}_{\text{noise}})$. This leads to the core relationship:

$$\text{Var}(\Delta \mathbf{v}_{\text{noise}}) \propto \epsilon_s \Delta t \tag{B2}$$

This shows that for the rate of energy injection to be constant, the variance of the kick added at each step must be directly proportional to the timestep Δt.

The magnitude of the random kick implemented in the code corresponds to its standard deviation, which is the square root of the variance. Therefore, the magnitude must scale with the square root of the timestep:

$$\text{Magnitude of kick} = \text{StdDev}(\Delta \mathbf{v}_{\text{noise}}) \propto \sqrt{\epsilon_s \Delta t} \propto \sqrt{\Delta t} \tag{B3}$$

This is why the stochastic term is implemented as $\Delta \mathbf{v}_{\text{noise}} = A(z) \cdot \sigma_v \cdot \sqrt{\Delta t} \cdot \mathcal{N}(0,1)$, where the stochastic intensity parameter σ_v is physically related to the TKE injection rate. This scaling ensures that the total stochastic energy added over a given period (e.g., one hour) is a physical constant and does not depend on our numerical choice of Δt. This is a standard result in the numerical integration of stochastic differential equations.

Author contributions. Hai Bui conceptualized the study, developed the code, conducted the simulations and analysis, and prepared the original draft. Mostafa Bakhoday-Paskyabi and Joachim Reuder contributed to the refinement of the methodology and interpretation of the results, and critically reviewed and edited the manuscript.

Competing interests. The authors declare that they have no competing interests.

https://doi.org/10.5194/wes-2026-66
Preprint. Discussion started: 23 April 2026

Acknowledgements. This work was supported by the Research Council of Norway (Norges forskningsråd) under the project ImpactWind SørVest (Grant No. 332034). The authors acknowledge the use of AI tools to assist with language editing and refinement.

https://doi.org/10.5194/wes-2026-66
Preprint. Discussion started: 23 April 2026

eawe european academy of wind energy
Open Access WIND ENERGY SCIENCE DISCUSSIONS

References

Boyer, C. H. and Keeler, J. M.: Evaluation and improvement of an inflow-nudging technique for idealized simulations of convective boundary layers, Journal of Applied Meteorology and Climatology, 61, 1843–1860, 2022.

Bui, H.: WRF-SADLES: Version 2.0b on Zenodo, https://doi.org/10.5281/zenodo.19591182, 2026a.

Bui, H.: haibuihoang/Dynamic-Geostrophic-Nudging: V1.0: Initial Release - 1D Demonstration of Dynamic Geostrophic Nudging (DGN), https://doi.org/10.5281/zenodo.19592301, 2026b.

Bui, H., Bakhoday-Paskyabi, M., and Mohammadpour-Penchah, M.: Implementation of a Simple Actuator Disk for Large-Eddy Simulation in the Weather Research and Forecasting Model (WRF-SADLES v1. 2) for wind turbine wake simulation, Geoscientific Model Development, 17, 4447–4465, 2024.

Dai, C., Wang, Q., Kalogiros, J., Lenschow, D., Gao, Z., and Zhou, M.: Determining boundary-layer height from aircraft measurements, Boundary-layer meteorology, 152, 277–302, 2014.

de Roode, S. R., Duynkerke, P. G., and Jonker, H. J.: Large-eddy simulation: How large is large enough?, Journal of the atmospheric sciences, 61, 403–421, 2004.

Garratt, J. R.: The atmospheric boundary layer, Earth-Science Reviews, 37, 89–134, 1994.

Grylls, T., Suter, I., and van Reeuwijk, M.: Steady-state large-eddy simulations of convective and stable urban boundary layers, Boundary-Layer Meteorology, 175, 309–341, 2020.

Jiménez, P. A., Dudhia, J., González-Rouco, J. F., Navarro, J., Montávez, J. P., and García-Bustamante, E.: A revised scheme for the WRF surface layer formulation, Monthly weather review, 140, 898–918, 2012.

Kale, B., Buckingham, S., van Beeck, J., and Cuerva-Tejero, A.: Implementation of a generalized actuator disk model into WRF v4. 3: A validation study for a real-scale wind turbine, Renewable Energy, 197, 810–827, 2022.

Lilly, D. K.: The representation of small-scale turbulence in numerical simulation experiments, IBM Form, pp. 195–210, 1967.

Meneveau, C. and Katz, J.: Scale-invariance and turbulence models for large-eddy simulation, Annual Review of Fluid Mechanics, 32, 1–32, 2000.

Mirocha, J. D., Lundquist, J. K., and Kosović, B.: Implementation of a large-eddy simulation mode into the Weather Research and Forecasting model, Monthly Weather Review, 142, 806–824, 2014.

Moeng, C.-H.: A large-eddy-simulation model for the study of planetary boundary-layer turbulence, Journal of the Atmospheric Sciences, 41, 2052–2062, https://doi.org/10.1175/1520-0469(1984)041<2052:ALESMF>2.0.CO;2, 1984.

Muñoz-Esparza, D., Lundquist, J. K., Sauer, J. A., Kosović, B., and Linn, R. R.: Bridging the transition from mesoscale to microscale turbulence in numerical weather prediction models, Boundary-Layer Meteorology, 162, 3–24, 2017.

Porté-Agel, F., Bastankhah, M., and Shamsoddin, S.: Wind-energy fluid mechanics turbulence models: A review, Boundary-Layer Meteorology, 174, 1–59, 2020.

Schnierstein, N., Chylik, J., Shupe, M. D., and Neggers, R.: Standardized daily high-resolution large-eddy simulations of the Arctic boundary layer and clouds during the complete MOSAiC drift, Journal of Advances in Modeling Earth Systems, 16, e2024MS004 296, 2024.

Skamarock, W. C., Klemp, J. B., Dudhia, J., Gill, D. O., Liu, Z., Berner, J., Wang, W., Powers, J. G., Duda, M. G., Barker, D. M., et al.: A description of the advanced research WRF version 4, NCAR tech. note ncar/tn-556+ str, 145, https://doi.org/10.5065/1dfh-6p97, 2019.

Stoll, R., Gibbs, J. A., Salesky, S. T., Anderson, W., and Calaf, M.: Large-eddy simulation of the atmospheric boundary layer, Boundary-Layer Meteorology, 177, 541–581, 2020.

https://doi.org/10.5194/wes-2026-66
Preprint. Discussion started: 23 April 2026

Stull, R. B.: An introduction to boundary layer meteorology, vol. 13, Springer Science & Business Media, https://doi.org/10.1007/978-94-009-3027-8, 2012.

Wrba, L., Englberger, A., Dörnbrack, A., Kilroy, G., and Wildmann, N.: Data assimilation of generic boundary layer flows for wind turbine applications–an LES study, Wind Energy Science, 10, 2217–2236, 2025.

Wyngaard, J. C.: Turbulence in the Atmosphere, Cambridge University Press, https://doi.org/10.1017/CBO9780511840524, 2010.